

## Scientific Inquiry and Review (SIR)

Volume 8 Issue 4, 2024


ISSN(P): 2521-2427, ISSN(E): 2521-2435

Homepage: <https://journals.umt.edu.pk/index.php/SIR>



Article QR



- Title:** On the Study of Topological Indices of Drugs against COVID-19
- Author (s):** Bushra Nadeem<sup>1</sup>, Muazzam Ali<sup>1</sup>, M U Hashmi<sup>1</sup>, Abdul Manan<sup>1</sup>, Bagh Ali<sup>2</sup>, and Sidra Siddiqui<sup>1</sup>
- Affiliation (s):** <sup>1</sup>The Superior University, Lahore Pakistan  
<sup>2</sup>Harbin Institute of Technology, Shenzhen, China
- DOI:** <https://doi.org/10.32350/sir.84.03>
- History:** Received: 21 July 2024, Revised: 29 August, 2024, Accepted: September 03, 2024,  
Published: December 15, 2024
- Citation:** Nadeem B, Ali M, Hashmi MU, Manan A, Ali B, Siddiqui S. On the study of topological indices of drugs against COVID-19. *Sci Inq Rev.* 2024;8(4):50–79. <https://doi.org/10.32350/sir.84.03>
- Copyright:** © The Authors
- Licensing:**  This article is open access and is distributed under the terms of [Creative Commons Attribution 4.0 International License](https://creativecommons.org/licenses/by/4.0/)
- Conflict of Interest:** Author(s) declared no conflict of interest



UMT

A publication of  
The School of Science  
University of Management and Technology, Lahore, Pakistan

## On the Study of Topological Indices of Drugs against COVID-19

Bushra Nadeem<sup>1</sup>, Muazzam Ali<sup>1\*</sup>, and M U Hashmi<sup>1</sup>, Abdul Manan<sup>1</sup>, Bagh Ali<sup>2</sup>, and Sidra Siddiqui<sup>1</sup>

<sup>1</sup>Department of Basic Sciences, The Superior University, Lahore Pakistan

<sup>2</sup>School of Mechanical Engineering and Automation, Harbin Institute of Technology, Shenzhen, China

### ABSTRACT

A topological index (TI) is an analytical metric of the molecular structure derived from the corresponding molecular graph. A class of viruses known as coronaviruses is responsible for human upper respiratory tract infections. Several antiviral medications currently available in the market are efficient in managing COVID-19. These include ritonavir, arbidol, theaflavin, hydroxychloroquine, chloroquine, and remdesivir (GS-5734). In this study, a set of TIs for remdesivir (GS-5734), arbidol, theaflavin, ritonavir, chloroquine, and hydroxychloroquine are computed based on their respective molecular graphs. These indices comprise Nirmala leap index, modified Nirmala leap index, first inverse Nirmala index, and second inverse Nirmala index. Additionally, the calculated outcomes are plotted to see how they are affected by the relevant parameters. The analysis shows that the Nirmala leap index ( $NL(H)$ ) shows the highest value among the studied indices, with Ritonavir leading at 285.7254. Conversely, the modified Nirmala leap index ( $mNL(H)$ ) shows the lowest value of 18.1063 for chloroquine. These findings may offer assistance in the advancement of novel COVID-19 treatment drugs.

**Keywords:** antiviral drugs, first inverse Nirmala Index, modified Nirmala leap index, Nirmala leap index, second inverse Nirmala index

### Highlights

- Computing TIs of the various drugs of COVID-19.
- Evaluating these indices to analyze and find the efficacy of these drugs in the treatment and management of COVID-19, showcasing how molecular shape affects antiviral activity.

---

\*Corresponding Author: [muazzamali@superior.edu.pk](mailto:muazzamali@superior.edu.pk)

- Use of molecular graphs and edge partitioning to visually represent and analyze the molecular systems of these drugs, thus enhancing the understanding of their chemical behaviours.

## 1.INTRODUCTION

Millions of people have died due to several infectious illnesses and epidemics throughout the course of history. The most deadly were the pandemics brought on by flu, cholera, plague, and other similar illnesses. The current COVID-19 pandemic has affected the health of people adversely, worldwide [1]. The coronavirus that causes COVID-19 is a novel betacoronavirus which is similar to previously reported MERS-CoV and SARS-CoV, in terms of both genetic sequence and viral structure.

Measuring the efficacy of the existing antiviral drugs in treating analogous viral infections comprises a useful drug discovery experiment. During the COVID-19 pandemic, the researchers examined selected antiviral medications available in the market *in vitro* and discovered that they were successful in preventing the infection and spread of COVID-19 [2–6]. These antiviral medications included remdesivir (GS-5734), arbidol, ritonavir, theaflavin, chloroquine, and hydroxychloroquine. A universal nucleotide analog drug called remdesivir was created to stop the spread of the Ebola virus [7, 8]. It also works well *in vitro* against COVID-19 [5, 9]. Numerous hospitals have conducted clinical research, although efficacy tests are still pending. A universal antiviral drug known as chloroquine is used to treat autoimmune illnesses, including malaria [10, 11]. Several randomized controlled studies have strived to know how well chloroquine works to treat COVID-19. Treatment benefits include lowered fever, improved CT imaging, and postponed onset of the illness [12].

The antiviral properties of chloroquine and hydroxychloroquine are strikingly similar. Since they have the capacity to impact the immune system, both may be more effective against viruses *in vivo*. Chloroquine and hydroxychloroquine have been cleared by the FDA (Food and Drug Authority) for use as emergency coronavirus treatments, according to a March 30, 2020 *Forbes* story. Hydroxychloroquine lessens the cytokine storm and shortens the early course of COVID-19 by inhibiting T cell activation [13, 14].

The health benefits of black tea have been associated with the polyphenol compound theaflavin. This compound shows antiviral efficacy

against a range of viruses, including influenza A, B, and C [15, 16]. Wiener discovered that theaflavin may be utilized as a starting point to prepare a COVID-19 inhibitor [17].

Both arbidol and ritonavir function as virus inhibitors, limiting its spread. A basic linked graph, with atoms and chemical bonds as nodes and edges, is called a molecular graph [18, 19]. The application of topological indices (TIs) in chemical graph theory to evaluate molecular properties has been the subject of numerous investigations. For example, Kulli [20] introduced the Nirmala index and also how to use it to assess the structural properties of nanostructures, emphasizing how well it predicts the stability of molecules. In their thorough analysis of mathematical ideas in organic chemistry, Gutman and Polansky, emphasized the significance of TIs in comprehending molecular interactions and for forecasting chemical behavior [21]. Furthermore, the application of TIs in determining the correlation of molecular structure with boiling points, a crucial component of Quantitative Structure-Property Relationship (QSPR) analysis, was made possible by Wiener's (1947) work on structural determination of paraffin boiling points [22].

TIs are invariant under graph isomorphisms, which are mathematical metrics of molecular graphs. In 1947, Wiener introduced the concept of first TI [17]. Physicochemical properties such as surface area, heat of formation, vapour pressure, surface tension, boiling points, and the boiling activities of the related chemical molecules can be examined using TIs. There are three different kinds of TIs, namely surface-based, degree-based, and distance-based TIs [20, 23, 24]. To examine molecular structure, chemical graph theory employs TIs such as the Nirmala index and its variants, namely the modified Nirmala leap index, first inverse Nirmala index, and second inverse Nirmala index [25]. These indices provide information about the general structure, stability, and reactivity of molecules by calculating the degrees of neighboring vertices in order to measure the connectivity of a graph. Nirmala index variants are useful tools to forecast chemical properties and investigate molecular behaviour because they offer a deeper understanding of various graph features, such as sparsity or the presence of particular substructures.

## 2. METHODOLOGY

TIs of various antiviral medication structures are among the primary discoveries of this research. To reach the conclusions, a network was created using molecular compounds and each vertex and edge was counted. Secondly, based on the degrees of the end vertices, the graphs' edge set was divided into several types. To obtain the intended conclusion, Nirmala leap index, modified Nirmala leap index, first inverse Nirmala index, and second inverse Nirmala index were used.

Let  $H$  be a finite, simple, connected graph using the edge set  $E(H)$  and vertex set  $V(H)$ . The number of edges incident to a vertex  $s$  is its degree or  $d(s)$ . The number of edges in the shortest path connecting any two vertices, namely  $s$  and  $t$  of  $H$ , is indicated by the distance between these two vertices, given by the formula  $d(s, t)$ . The  $k$ -th open neighborhood of  $t$  in  $H$ , given a positive integer  $k$  and  $t \in V(H)$ , is defined as  $N_k(t/H) = \{s \in V(H) : d(s, t) = k\}$ . The number of  $t$ 's  $k$ -neighbors in  $H$  is its  $k$ -distance degree and it is represented by  $d_k(t)$ .

Kulli [26] presented the Nirmala index of a graph  $H$  as follows:

$$N(H) = \sum_{st \in E(H)} [d(s) + d(t)]1/2$$

Some types of Nirmala indices were studied recently, for example, in [26, 27]. We present the definition of the Nirmala leap index of a graph  $H$ , which is

$$NL(H) = \sum_{st \in E(H)} [d(s) + d(t)]1/2. \tag{2.1}$$

A few leap indices were recently examined, for example, in [28, 29]. For a graph  $H$ , its modified Nirmala leap index is defined as follows:

$$mNL(H) = \sum_{st \in E(H)} \frac{1}{\sqrt{d(s)+d(t)}}. \tag{2.2}$$

Eventually, in 2021, Kulli [30] defined the first and second inverse Nirmala indices of a molecular graph  $H$  as follows:

$$IN1(H) = \sum_{st \in E(H)} \sqrt{\frac{1}{d(s)} + \frac{1}{d(t)}} = \sum_{st \in E(H)} \left(\frac{1}{d(s)} + \frac{1}{d(t)}\right)^{\frac{1}{2}}, \tag{2.3}$$

$$IN2(H) = \sum_{st \in E(H)} \frac{1}{\sqrt{\frac{1}{d(s)} + \frac{1}{d(t)}}} = \sum_{st \in E(H)} \left(\frac{1}{d(s)} + \frac{1}{d(t)}\right)^{-\frac{1}{2}}. \tag{2.4}$$

In this paper, we compute the Nirmala leap index, modified Nirmala leap index, first inverse Nirmala index, and second inverse Nirmala index for arbidol, remdesivir (GS-5734), theaflavin, ritonavir, chloroquine, and hydroxychloroquine.

### 3. RESULTS AND DISCUSSION

#### 3.1. Remdesivir (GS-5734)

Remdesivir is an all-around antiviral medication first created to treat hepatitis C. It is currently administered to treat COVID-19 after therapy. Figure 1 displays its molecular graph and Table 1 demonstrates its edge partition according to degree. This structure has 41 vertices and 44 edges (see Figure 1).

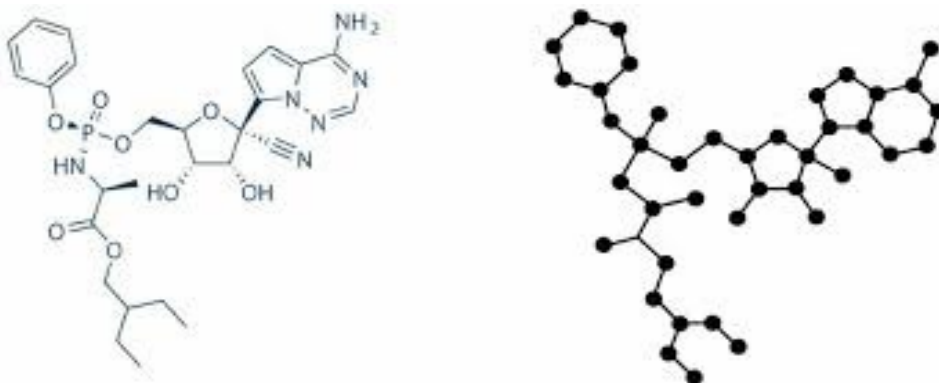


**Figure 1.** Remdesivir's Molecular Grap

**Table 1.** Edge Partitioning of Remdesivir Based on Degree

$(d_2(s), d_2(t))$	Frequency
(1,2)	2
(1,3)	5
(1,4)	2
(2,2)	9
(2,3)	14
(2,4)	6
(3,3)	6
(3,4)	2
(3,6)	3
(3,7)	1
(3,8)	1

$(d_2(s), d_2(t))$	Frequency
(4,4)	2
(4,5)	4
(4,6)	2
(4,7)	1
(4,9)	1
(5,5)	2
(5,6)	6
(5,7)	1
(5,8)	2
(5,9)	1
(6,6)	1
(6,7)	3
(6,8)	1
(7,7)	4
(7,8)	1
(7,9)	1
(8,8)	1
(8,9)	2
(9,9)	1

**Theorem 3.1.** Nirmala leap index, modified Nirmala leap index, first inverse Nirmala index, and second inverse Nirmala index for remdesivir are as follows:

- a)  $NL(H) = 246.3012,$
- b)  $mNL(H) = 33.3229,$
- c)  $IN1(H) = 69.0372,$
- d)  $IN2(H) = 119.9954.$

**Proof.** By using the degree-based edge partition and definitions, we may conclude that

$$\begin{aligned}
 \text{a) } NL(H) = \sum_{st \in E(H)} [d(s) + d(t)]^{1/2} = & 2(1 + 2)^{1/2} + 5(1 + 3)^{1/2} + \\
 & 2(1 + 4)^{1/2} + 9(2 + 2)^{1/2} + 14(2 + 3)^{1/2} + 6(2 + 4)^{1/2} + 6(3 + \\
 & 3)^{1/2} + 2(3 + 4)^{1/2} + 3(3 + 6)^{1/2} + 1(3 + 7)^{1/2} + 1(3 + 8)^{1/2} + 2(4 + \\
 & 4)^{1/2} + 4(4 + 5)^{1/2} + 2(4 + 6)^{1/2} + 1(4 + 7)^{1/2} + 1(4 + 9)^{1/2} + 2(5 + \\
 & 5)^{1/2} + 6(5 + 6)^{1/2} + 1(5 + 7)^{1/2} + 2(5 + 8)^{1/2} + 1(5 + 9)^{1/2} + 1(6 +
 \end{aligned}$$

$$6)^{1/2} + 3(6 + 7)^{1/2} + 1(6 + 8)^{1/2} + 4(7 + 7)^{1/2} + 1(7 + 8)^{1/2} + 1(7 + 9)^{1/2} + 1(8 + 8)^{1/2} + 2(8 + 9)^{1/2} + 1(9 + 9)^{1/2} = 246.3012.$$

$$\begin{aligned} \text{b) } mNL(H) &= \sum_{st \in E(H)} \frac{1}{\sqrt{d(s)+d(t)}} = 2(1 + 2)^{-1/2} + 5(1 + 3)^{-1/2} + 2(1 + 4)^{-1/2} + 9(2 + 2)^{-1/2} + 14(2 + 3)^{-1/2} + 6(2 + 4)^{-1/2} + 6(3 + 3)^{-1/2} + 2(3 + 4)^{-1/2} + 3(3 + 6)^{-1/2} + 1(3 + 7)^{-1/2} + 1(3 + 8)^{-1/2} + 2(4 + 4)^{-1/2} + 4(4 + 5)^{-1/2} + 2(4 + 6)^{-1/2} + 1(4 + 7)^{-1/2} + 1(4 + 9)^{-1/2} + 2(5 + 5)^{-1/2} + 6(5 + 6)^{-1/2} + 1(5 + 7)^{-1/2} + 2(5 + 8)^{-1/2} + 1(5 + 9)^{-1/2} + 1(6 + 6)^{-1/2} + 3(6 + 7)^{-1/2} + 1(6 + 8)^{-1/2} + 4(7 + 7)^{-1/2} + 1(7 + 8)^{-1/2} + 1(7 + 9)^{-1/2} + 1(8 + 8)^{-1/2} + 2(8 + 9)^{-1/2} + 1(9 + 9)^{-1/2} \\ &= 33.3229. \end{aligned}$$

$$\begin{aligned} \text{c) } IN1(H) &= \sum_{st \in E(H)} \left( \frac{1}{d(s)} + \frac{1}{d(t)} \right)^{\frac{1}{2}} = 2 \left( \frac{1}{1} + \frac{1}{2} \right)^{\frac{1}{2}} + 5 \left( \frac{1}{1} + \frac{1}{3} \right)^{\frac{1}{2}} + 2 \left( \frac{1}{1} + \frac{1}{4} \right)^{\frac{1}{2}} + 9 \left( \frac{1}{2} + \frac{1}{2} \right)^{\frac{1}{2}} + 14 \left( \frac{1}{2} + \frac{1}{3} \right)^{\frac{1}{2}} + 6 \left( \frac{1}{2} + \frac{1}{4} \right)^{\frac{1}{2}} + 6 \left( \frac{1}{3} + \frac{1}{3} \right)^{\frac{1}{2}} + 2 \left( \frac{1}{3} + \frac{1}{4} \right)^{\frac{1}{2}} + 3 \left( \frac{1}{3} + \frac{1}{6} \right)^{\frac{1}{2}} + 1 \left( \frac{1}{3} + \frac{1}{7} \right)^{\frac{1}{2}} + 1 \left( \frac{1}{3} + \frac{1}{8} \right)^{\frac{1}{2}} + 2 \left( \frac{1}{4} + \frac{1}{4} \right)^{\frac{1}{2}} + 4 \left( \frac{1}{4} + \frac{1}{5} \right)^{\frac{1}{2}} + 2 \left( \frac{1}{4} + \frac{1}{6} \right)^{\frac{1}{2}} + 1 \left( \frac{1}{4} + \frac{1}{7} \right)^{\frac{1}{2}} + 1 \left( \frac{1}{4} + \frac{1}{9} \right)^{\frac{1}{2}} + 2 \left( \frac{1}{5} + \frac{1}{5} \right)^{\frac{1}{2}} + 6 \left( \frac{1}{5} + \frac{1}{6} \right)^{\frac{1}{2}} + 1 \left( \frac{1}{5} + \frac{1}{7} \right)^{\frac{1}{2}} + 2 \left( \frac{1}{5} + \frac{1}{8} \right)^{\frac{1}{2}} + 1 \left( \frac{1}{5} + \frac{1}{9} \right)^{\frac{1}{2}} + 1 \left( \frac{1}{6} + \frac{1}{6} \right)^{\frac{1}{2}} + 3 \left( \frac{1}{6} + \frac{1}{7} \right)^{\frac{1}{2}} + 1 \left( \frac{1}{6} + \frac{1}{8} \right)^{\frac{1}{2}} + 4 \left( \frac{1}{7} + \frac{1}{7} \right)^{\frac{1}{2}} + 1 \left( \frac{1}{7} + \frac{1}{8} \right)^{\frac{1}{2}} + 1 \left( \frac{1}{7} + \frac{1}{9} \right)^{\frac{1}{2}} + 1 \left( \frac{1}{8} + \frac{1}{8} \right)^{\frac{1}{2}} + 2 \left( \frac{1}{8} + \frac{1}{9} \right)^{\frac{1}{2}} + 1 \left( \frac{1}{9} + \frac{1}{9} \right)^{\frac{1}{2}} = 69.0372. \end{aligned}$$

$$\begin{aligned} \text{d) } IN2(H) &= \sum_{st \in E(H)} \left( \frac{1}{d(s)} + \frac{1}{d(t)} \right)^{-\frac{1}{2}} = 2 \left( \frac{1}{1} + \frac{1}{2} \right)^{-\frac{1}{2}} + 5 \left( \frac{1}{1} + \frac{1}{3} \right)^{-\frac{1}{2}} + 2 \left( \frac{1}{1} + \frac{1}{4} \right)^{-\frac{1}{2}} + 9 \left( \frac{1}{2} + \frac{1}{2} \right)^{-\frac{1}{2}} + 14 \left( \frac{1}{2} + \frac{1}{3} \right)^{-\frac{1}{2}} + 6 \left( \frac{1}{2} + \frac{1}{4} \right)^{-\frac{1}{2}} + 6 \left( \frac{1}{3} + \frac{1}{3} \right)^{-\frac{1}{2}} + 2 \left( \frac{1}{3} + \frac{1}{4} \right)^{-\frac{1}{2}} + 3 \left( \frac{1}{3} + \frac{1}{6} \right)^{-\frac{1}{2}} + 1 \left( \frac{1}{3} + \frac{1}{7} \right)^{-\frac{1}{2}} + 1 \left( \frac{1}{3} + \frac{1}{8} \right)^{-\frac{1}{2}} + 2 \left( \frac{1}{4} + \frac{1}{4} \right)^{-\frac{1}{2}} + 4 \left( \frac{1}{4} + \frac{1}{5} \right)^{-\frac{1}{2}} + 2 \left( \frac{1}{4} + \frac{1}{6} \right)^{-\frac{1}{2}} + 1 \left( \frac{1}{4} + \frac{1}{7} \right)^{-\frac{1}{2}} + 1 \left( \frac{1}{4} + \frac{1}{9} \right)^{-\frac{1}{2}} + 2 \left( \frac{1}{5} + \frac{1}{5} \right)^{-\frac{1}{2}} + 6 \left( \frac{1}{5} + \frac{1}{6} \right)^{-\frac{1}{2}} + 1 \left( \frac{1}{5} + \frac{1}{7} \right)^{-\frac{1}{2}} + 2 \left( \frac{1}{5} + \frac{1}{8} \right)^{-\frac{1}{2}} + 1 \left( \frac{1}{5} + \frac{1}{9} \right)^{-\frac{1}{2}} + 1 \left( \frac{1}{6} + \frac{1}{6} \right)^{-\frac{1}{2}} + 3 \left( \frac{1}{6} + \frac{1}{7} \right)^{-\frac{1}{2}} + 1 \left( \frac{1}{6} + \frac{1}{8} \right)^{-\frac{1}{2}} + 4 \left( \frac{1}{7} + \frac{1}{7} \right)^{-\frac{1}{2}} + 1 \left( \frac{1}{7} + \frac{1}{8} \right)^{-\frac{1}{2}} + 1 \left( \frac{1}{7} + \frac{1}{9} \right)^{-\frac{1}{2}} + 1 \left( \frac{1}{8} + \frac{1}{8} \right)^{-\frac{1}{2}} + 2 \left( \frac{1}{8} + \frac{1}{9} \right)^{-\frac{1}{2}} + 1 \left( \frac{1}{9} + \frac{1}{9} \right)^{-\frac{1}{2}} = 119.9954. \end{aligned}$$



### 3.2. Chloroquine

Malaria is treated with chloroquine. Early in the pandemic, it was investigated as a treatment for COVID-19. However, research on its usage was mostly abandoned in the summer of 2020 and it is no longer advised. It is consumed orally. Common side effects include rash, diarrhea, loss of appetite, and muscle pain. Figure 2 displays chloroquine's molecular graph. Table 2 demonstrates the edge partition according to degree. This structure has 21 vertices and 23 edges (see Figure 2).

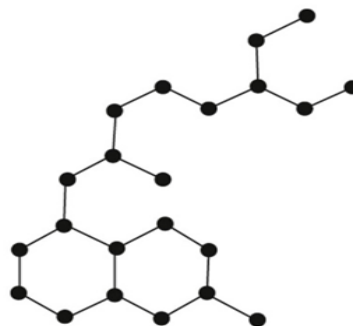
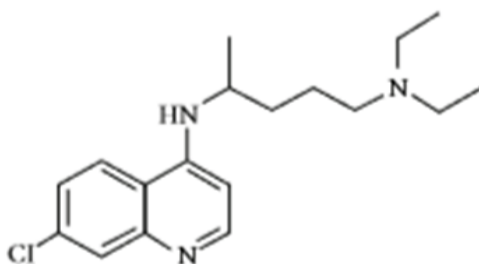


**Figure 2.** Chloroquine's Molecular Graph

**Table 2.** Edge Partitioning of Chloroquine Based on Degree

$(d_2(s), d_2(t))$	Frequency
(1,2)	2
(1,3)	2
(2,2)	5
(2,3)	12
(3,3)	2
(2,4)	2
(3,5)	2
(4,5)	4
(4,6)	2
(5,5)	3
(5,6)	3
(5,7)	2
(5,8)	1
(6,7)	2
(7,8)	2

**Theorem 3.2.** Nirmala leap index, Modified Nirmala leap index, first inverse Nirmala index, and second inverse Nirmala index for chloroquine are as follows:

- a)  $NL(H) = 123.004$ ,
- b)  $mNL(H) = 18.1063$ ,
- c)  $IN1(H) = 37.1161$ ,
- d)  $IN2(H) = 60.3967$ .

**Proof.** By using the degree-based edge partition and definitions, we may conclude that

- a) 
$$NL(H) = \sum_{st \in E(H)} [d(s) + d(t)]^{1/2} = 2(1 + 2)^{1/2} + 2(1 + 3)^{1/2} + 5(2 + 2)^{1/2} + 12(2 + 3)^{1/2} + 2(3 + 3)^{1/2} + 2(2 + 4)^{1/2} + 2(3 + 5)^{1/2} + 4(4 + 5)^{1/2} + 2(4 + 6)^{1/2} + 3(5 + 5)^{1/2} + 3(5 + 6)^{1/2} + 2(5 + 7)^{1/2} + 1(5 + 8)^{1/2} + 2(6 + 7)^{1/2} + 2(7 + 8)^{1/2} = 123.004.$$
- b) 
$$mNL(H) = \sum_{st \in E(H)} \frac{1}{\sqrt{d(s)+d(t)}} = 2(1 + 2)^{-1/2} + 2(1 + 3)^{-1/2} + 5(2 + 2)^{-1/2} + 12(2 + 3)^{-1/2} + 2(3 + 3)^{-1/2} + 2(2 + 4)^{-1/2} + 2(3 + 5)^{-1/2} + 4(4 + 5)^{-1/2} + 2(4 + 6)^{-1/2} + 3(5 + 5)^{-1/2} + 3(5 + 6)^{-1/2} + 2(5 + 7)^{-1/2} + 1(5 + 8)^{-1/2} + 2(6 + 7)^{-1/2} + 2(7 + 8)^{-1/2} = 18.1063.$$
- c) 
$$IN1(H) = \sum_{st \in E(H)} \left( \frac{1}{d(s)} + \frac{1}{d(t)} \right)^{\frac{1}{2}} = 2 \left( \frac{1}{1} + \frac{1}{2} \right)^{\frac{1}{2}} + 2 \left( \frac{1}{1} + \frac{1}{3} \right)^{\frac{1}{2}} + 5 \left( \frac{1}{2} + \frac{1}{2} \right)^{\frac{1}{2}} + 12 \left( \frac{1}{2} + \frac{1}{3} \right)^{\frac{1}{2}} + 2 \left( \frac{1}{3} + \frac{1}{3} \right)^{\frac{1}{2}} + 2 \left( \frac{1}{2} + \frac{1}{4} \right)^{\frac{1}{2}} + 2 \left( \frac{1}{3} + \frac{1}{5} \right)^{\frac{1}{2}} + 4 \left( \frac{1}{4} + \frac{1}{5} \right)^{\frac{1}{2}} + 2 \left( \frac{1}{4} + \frac{1}{6} \right)^{\frac{1}{2}} + 3 \left( \frac{1}{5} + \frac{1}{5} \right)^{\frac{1}{2}} + 3 \left( \frac{1}{5} + \frac{1}{6} \right)^{\frac{1}{2}} + 2 \left( \frac{1}{5} + \frac{1}{7} \right)^{\frac{1}{2}} + 1 \left( \frac{1}{5} + \frac{1}{8} \right)^{\frac{1}{2}} + 2 \left( \frac{1}{6} + \frac{1}{7} \right)^{\frac{1}{2}} + 2 \left( \frac{1}{7} + \frac{1}{8} \right)^{\frac{1}{2}} = 37.1161.$$
- d) 
$$IN2(H) = \sum_{st \in E(H)} \left( \frac{1}{d(s)} + \frac{1}{d(t)} \right)^{-\frac{1}{2}} = 2 \left( \frac{1}{1} + \frac{1}{2} \right)^{-\frac{1}{2}} + 2 \left( \frac{1}{1} + \frac{1}{3} \right)^{-\frac{1}{2}} + 5 \left( \frac{1}{2} + \frac{1}{2} \right)^{-\frac{1}{2}} + 12 \left( \frac{1}{2} + \frac{1}{3} \right)^{-\frac{1}{2}} + 2 \left( \frac{1}{3} + \frac{1}{3} \right)^{-\frac{1}{2}} + 2 \left( \frac{1}{2} + \frac{1}{4} \right)^{-\frac{1}{2}} + 2 \left( \frac{1}{3} + \frac{1}{5} \right)^{-\frac{1}{2}} + 4 \left( \frac{1}{4} + \frac{1}{5} \right)^{-\frac{1}{2}} + 2 \left( \frac{1}{4} + \frac{1}{6} \right)^{-\frac{1}{2}} + 3 \left( \frac{1}{5} + \frac{1}{5} \right)^{-\frac{1}{2}} + 3 \left( \frac{1}{5} + \frac{1}{6} \right)^{-\frac{1}{2}} + 2 \left( \frac{1}{5} + \frac{1}{7} \right)^{-\frac{1}{2}} + 1 \left( \frac{1}{5} + \frac{1}{8} \right)^{-\frac{1}{2}} + 2 \left( \frac{1}{6} + \frac{1}{7} \right)^{-\frac{1}{2}} + 2 \left( \frac{1}{7} + \frac{1}{8} \right)^{-\frac{1}{2}} = 60.3967.$$

### 3.3. Hydroxychloroquine

Hydroxychloroquine is an antimalarial medication administered in regions where chloroquine-sensitive malaria persists. It is often administered orally as hydroxychloroquine sulfate. Research has been conducted on the potential of hydroxychloroquine to prevent and treat COVID-19. Figure 3 displays hydroxychloroquine's molecular graph. Table 3 demonstrates the edge partition according to degree. This structure has 22 vertices and 24 edges (see Figure 3).

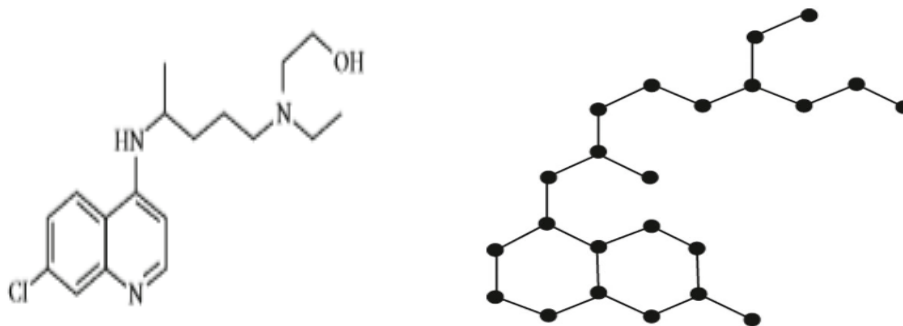


**Figure 3.** Hydroxychloroquine's Molecular Graph

**Table 3.** Edge Partitioning of Hydroxychloroquine Based on Degree

$(d_2(s), d_2(t))$	Frequency
(1,2)	2
(1,3)	2
(2,2)	6
(2,3)	13
(3,3)	2
(2,4)	1
(3,5)	3
(4,5)	4
(4,6)	1
(5,5)	3
(5,6)	4
(5,7)	2
(5,8)	1
(6,7)	2
(7,8)	2

**Theorem 3.3.** Nirmala leap index, modified Nirmala leap index, first inverse Nirmala index, and second inverse Nirmala index for hydroxychloroquine are as follows:

a)  $NL(H) = 127.7733$ ,

b)  $mNL(H) = 18.9840$ ,

c)  $IN1(H) = 38.8533$ ,

d)  $IN2(H) = 62.8089$ .

**Proof.** By using the degree-based edge partition and definitions, we may conclude that

a) 
$$NL(H) = \sum_{st \in E(H)} [d(s) + d(t)]1/2 = 2(1 + 2)^{1/2} + 2(1 + 3)^{1/2} + 6(2 + 2)^{1/2} + 13(2 + 3)^{1/2} + 2(3 + 3)^{1/2} + 1(2 + 4)^{1/2} + 3(3 + 5)^{1/2} + 4(4 + 5)^{1/2} + 1(4 + 6)^{1/2} + 3(5 + 5)^{1/2} + 4(5 + 6)^{1/2} + 2(5 + 7)^{1/2} + 1(5 + 8)^{1/2} + 2(6 + 7)^{1/2} + 2(7 + 8)^{1/2} = 127.7733.$$

b) 
$$mNL(H) = \sum_{st \in E(H)} \frac{1}{\sqrt{d(s)+d(t)}} = 2(1 + 2)^{-1/2} + 2(1 + 3)^{-1/2} + 6(2 + 2)^{-1/2} + 13(2 + 3)^{-1/2} + 2(3 + 3)^{-1/2} + 1(2 + 4)^{-1/2} + 3(3 + 5)^{-1/2} + 4(4 + 5)^{-1/2} + 1(4 + 6)^{-1/2} + 3(5 + 5)^{-1/2} + 4(5 + 6)^{-1/2} + 2(5 + 7)^{-1/2} + 1(5 + 8)^{-1/2} + 2(6 + 7)^{-1/2} + 2(7 + 8)^{-1/2} = 18.9840.$$

c) 
$$IN1(H) = \sum_{st \in E(H)} \left( \frac{1}{d(s)} + \frac{1}{d(t)} \right)^{\frac{1}{2}} = 2 \left( \frac{1}{1} + \frac{1}{2} \right)^{\frac{1}{2}} + 2 \left( \frac{1}{1} + \frac{1}{3} \right)^{\frac{1}{2}} + 6 \left( \frac{1}{2} + \frac{1}{2} \right)^{\frac{1}{2}} + 13 \left( \frac{1}{2} + \frac{1}{3} \right)^{\frac{1}{2}} + 2 \left( \frac{1}{3} + \frac{1}{3} \right)^{\frac{1}{2}} + 1 \left( \frac{1}{2} + \frac{1}{4} \right)^{\frac{1}{2}} + 3 \left( \frac{1}{3} + \frac{1}{5} \right)^{\frac{1}{2}} + 4 \left( \frac{1}{4} + \frac{1}{5} \right)^{\frac{1}{2}} + 1 \left( \frac{1}{4} + \frac{1}{6} \right)^{\frac{1}{2}} + 3 \left( \frac{1}{5} + \frac{1}{5} \right)^{\frac{1}{2}} + 4 \left( \frac{1}{5} + \frac{1}{6} \right)^{\frac{1}{2}} + 2 \left( \frac{1}{5} + \frac{1}{7} \right)^{\frac{1}{2}} + 1 \left( \frac{1}{5} + \frac{1}{8} \right)^{\frac{1}{2}} + 2 \left( \frac{1}{6} + \frac{1}{7} \right)^{\frac{1}{2}} + 2 \left( \frac{1}{7} + \frac{1}{8} \right)^{\frac{1}{2}} = 38.8533.$$

d) 
$$IN2(H) = \sum_{st \in E(H)} \left( \frac{1}{d(s)} + \frac{1}{d(t)} \right)^{-\frac{1}{2}} = 2 \left( \frac{1}{1} + \frac{1}{2} \right)^{-\frac{1}{2}} + 2 \left( \frac{1}{1} + \frac{1}{3} \right)^{-\frac{1}{2}} + 6 \left( \frac{1}{2} + \frac{1}{2} \right)^{-\frac{1}{2}} + 13 \left( \frac{1}{2} + \frac{1}{3} \right)^{-\frac{1}{2}} + 2 \left( \frac{1}{3} + \frac{1}{3} \right)^{-\frac{1}{2}} + 1 \left( \frac{1}{2} + \frac{1}{4} \right)^{-\frac{1}{2}} + 3 \left( \frac{1}{3} + \frac{1}{5} \right)^{-\frac{1}{2}} + 4 \left( \frac{1}{4} + \frac{1}{5} \right)^{-\frac{1}{2}} + 1 \left( \frac{1}{4} + \frac{1}{6} \right)^{-\frac{1}{2}} + 3 \left( \frac{1}{5} + \frac{1}{5} \right)^{-\frac{1}{2}} + 4 \left( \frac{1}{5} + \frac{1}{6} \right)^{-\frac{1}{2}} + 2 \left( \frac{1}{5} + \frac{1}{7} \right)^{-\frac{1}{2}} + 1 \left( \frac{1}{5} + \frac{1}{8} \right)^{-\frac{1}{2}} + 2 \left( \frac{1}{6} + \frac{1}{7} \right)^{-\frac{1}{2}} + 2 \left( \frac{1}{7} + \frac{1}{8} \right)^{-\frac{1}{2}} = 62.8089.$$

### 3.4. Theaflavin

Black tea contains a class of polyphenolic chemicals called theaflavins, which remain interesting due to their possible health advantages, including antiviral capabilities. Figure 4 displays theaflavin's molecular graph. Table 4 demonstrates the edge partition according to degree. This structure has 41 vertices and 46 edges (see Figure 4).

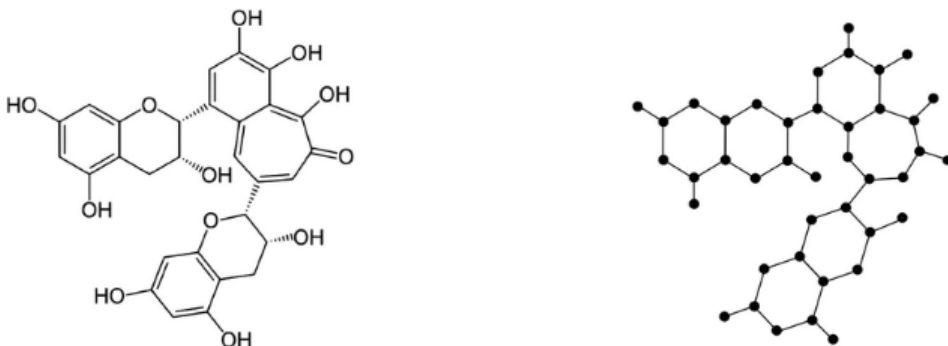


**Figure 4.** Theaflavin 's Molecular Graph

**Table 4.** Edge Partitioning of Theaflavin Based on Degree

$(d_2(s), d_2(t))$	Frequency
(1,3)	10
(2,3)	22
(3,3)	14
(3,5)	2
(3,6)	6
(3,7)	2
(5,6)	4
(6,6)	6
(6,7)	8
(6,8)	10
(7,8)	3
(7,9)	2
(8,8)	2
(8,9)	1

**Theorem 3.4.** Nirmala leap index, Modified Nirmala leap index, first inverse Nirmala index, and second inverse Nirmala index for theaflavin are as follows:

a)  $NL(H) = 265.5221$ ,

b)  $mNL(H) = 33.7404$ ,

c)  $IN1(H) = 69.9288$ ,

d)  $IN2(H) = 129.7463$ .

**Proof.** By using the degree-based edge partition and definitions, we may conclude that

a) 
$$NL(H) = \sum_{st \in E(H)} [d(s) + d(t)]^{1/2} = 10(1 + 3)^{1/2} + 22(2 + 3)^{1/2} + 14(3 + 3)^{1/2} + 2(3 + 5)^{1/2} + 6(3 + 6)^{1/2} + 2(3 + 7)^{1/2} + 4(5 + 6)^{1/2} + 6(6 + 6)^{1/2} + 8(6 + 7)^{1/2} + 10(6 + 8)^{1/2} + 3(7 + 8)^{1/2} + 2(7 + 9)^{1/2} + 2(8 + 8)^{1/2} + 1(8 + 9)^{1/2} = 265.5221$$

b) 
$$mNL(H) = \sum_{st \in E(H)} \frac{1}{\sqrt{d(s)+d(t)}} = 10(1 + 3)^{-1/2} + 22(2 + 3)^{-1/2} + 14(3 + 3)^{-1/2} + 2(3 + 5)^{-1/2} + 6(3 + 6)^{-1/2} + 2(3 + 7)^{-1/2} + 4(5 + 6)^{-1/2} + 6(6 + 6)^{-1/2} + 8(6 + 7)^{-1/2} + 10(6 + 8)^{-1/2} + 3(7 + 8)^{-1/2} + 2(7 + 9)^{-1/2} + 2(8 + 8)^{-1/2} + 1(8 + 9)^{-1/2} = 33.7404$$

c) 
$$IN1(H) = \sum_{st \in E(H)} \left(\frac{1}{d(s)} + \frac{1}{d(t)}\right)^{\frac{1}{2}} = 10\left(\frac{1}{1} + \frac{1}{3}\right)^{\frac{1}{2}} + 22\left(\frac{1}{2} + \frac{1}{3}\right)^{\frac{1}{2}} + 14\left(\frac{1}{3} + \frac{1}{3}\right)^{\frac{1}{2}} + 2\left(\frac{1}{3} + \frac{1}{5}\right)^{\frac{1}{2}} + 6\left(\frac{1}{3} + \frac{1}{6}\right)^{\frac{1}{2}} + 2\left(\frac{1}{3} + \frac{1}{7}\right)^{\frac{1}{2}} + 4\left(\frac{1}{5} + \frac{1}{6}\right)^{\frac{1}{2}} + 6\left(\frac{1}{6} + \frac{1}{6}\right)^{\frac{1}{2}} + 8\left(\frac{1}{6} + \frac{1}{7}\right)^{\frac{1}{2}} + 10\left(\frac{1}{6} + \frac{1}{8}\right)^{\frac{1}{2}} + 3\left(\frac{1}{7} + \frac{1}{8}\right)^{\frac{1}{2}} + 2\left(\frac{1}{7} + \frac{1}{9}\right)^{\frac{1}{2}} + 2\left(\frac{1}{8} + \frac{1}{8}\right)^{\frac{1}{2}} + 1\left(\frac{1}{8} + \frac{1}{9}\right)^{\frac{1}{2}} = 69.9288$$

d) 
$$IN2(H) = \sum_{st \in E(H)} \left(\frac{1}{d(s)} + \frac{1}{d(t)}\right)^{-\frac{1}{2}} = 10\left(\frac{1}{1} + \frac{1}{3}\right)^{-\frac{1}{2}} + 22\left(\frac{1}{2} + \frac{1}{3}\right)^{-\frac{1}{2}} + 14\left(\frac{1}{3} + \frac{1}{3}\right)^{-\frac{1}{2}} + 2\left(\frac{1}{3} + \frac{1}{5}\right)^{-\frac{1}{2}} + 6\left(\frac{1}{3} + \frac{1}{6}\right)^{-\frac{1}{2}} + 2\left(\frac{1}{3} + \frac{1}{7}\right)^{-\frac{1}{2}} + 4\left(\frac{1}{5} + \frac{1}{6}\right)^{-\frac{1}{2}} + 6\left(\frac{1}{6} + \frac{1}{6}\right)^{-\frac{1}{2}} + 8\left(\frac{1}{6} + \frac{1}{7}\right)^{-\frac{1}{2}} + 10\left(\frac{1}{6} + \frac{1}{8}\right)^{-\frac{1}{2}} + 3\left(\frac{1}{7} + \frac{1}{8}\right)^{-\frac{1}{2}} + 2\left(\frac{1}{7} + \frac{1}{9}\right)^{-\frac{1}{2}} + 2\left(\frac{1}{8} + \frac{1}{8}\right)^{-\frac{1}{2}} + 1\left(\frac{1}{8} + \frac{1}{9}\right)^{-\frac{1}{2}} = 129.7463$$

### 3.5. Ritonavir

A bioactive protein inhibitor medication called ritonavir is used to treat viruses. It produces noninfectious viruses by causing deregulation in the structure and functional proteins of the virus. It demonstrated antiviral action against the main coronavirus types that infected the human respiratory system. Ritonavir is often used for COVID-19 that is mild to moderate. Figure 5 displays ritonavir's molecular graph. Table 5 demonstrates the edge partition according to degree. This structure has 50 vertices and 53 edges (see Figure 5).

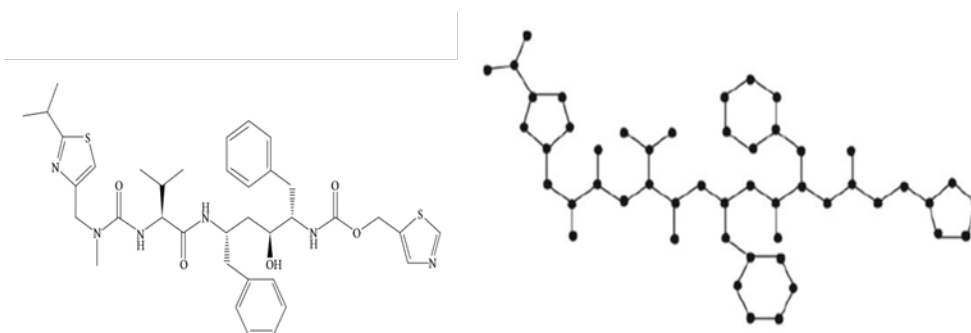


**Figure 5.** Ritonavir 's Molecular Graph

**Table 5.** Edge Partitioning of Ritonavir Based on Degree

$(d_2(s), d_2(t))$	Frequency
(1,3)	9
(2,2)	13
(2,3)	26
(3,3)	5
(3,5)	5
(4,4)	5
(3,6)	4
(4,5)	6
(5,5)	3
(5,6)	10
(5,7)	3
(6,6)	11
(5,8)	1
(6,7)	3
(6,8)	2

**Theorem 3.5.** Nirmala leap index, modified Nirmala leap index, first inverse Nirmala index, and second inverse Nirmala index for ritonavir are as follows:

a)  $NL(H) = 285.7254$ ,

b)  $mNL(H) = 41.1869$ ,

c)  $IN1(H) = 84.63$ ,

d)  $IN2(H) = 140.2006$ .

**Proof.** By using the degree-based edge partition and definitions, we may conclude that

a)  $NL(H) = \sum_{st \in E(H)} [d(s) + d(t)]1/2 = 9(1 + 3)^{1/2} + 13(2 + 2)^{1/2} + 26(2 + 3)^{1/2} + 5(3 + 3)^{1/2} + 5(3 + 5)^{1/2} + 5(4 + 4)^{1/2} + 4(3 + 6)^{1/2} + 6(4 + 5)^{1/2} + 3(5 + 5)^{1/2} + 10(5 + 6)^{1/2} + 3(5 + 7)^{1/2} + 11(6 + 6)^{1/2} + 1(5 + 8)^{1/2} + 3(6 + 7)^{1/2} + 2(6 + 8)^{1/2} = 285.7254$

b)  $mNL(H) = \sum_{st \in E(H)} \frac{1}{\sqrt{d(s)+d(t)}} = 9(1 + 3)^{-1/2} + 13(2 + 2)^{-1/2} + 26(2 + 3)^{-1/2} + 5(3 + 3)^{-1/2} + 5(3 + 5)^{-1/2} + 5(4 + 4)^{-1/2} + 4(3 + 6)^{-1/2} + 6(4 + 5)^{-1/2} + 3(5 + 5)^{-1/2} + 10(5 + 6)^{-1/2} + 3(5 + 7)^{-1/2} + 11(6 + 6)^{-1/2} + 1(5 + 8)^{-1/2} + 3(6 + 7)^{-1/2} + 2(6 + 8)^{-1/2} = 41.1869$

c)  $IN1(H) = \sum_{st \in E(H)} \left( \frac{1}{d(s)} + \frac{1}{d(t)} \right)^{\frac{1}{2}} = 9 \left( \frac{1}{1} + \frac{1}{3} \right)^{\frac{1}{2}} + 13 \left( \frac{1}{2} + \frac{1}{2} \right)^{\frac{1}{2}} + 26 \left( \frac{1}{2} + \frac{1}{3} \right)^{\frac{1}{2}} + 5 \left( \frac{1}{3} + \frac{1}{3} \right)^{\frac{1}{2}} + 5 \left( \frac{1}{3} + \frac{1}{5} \right)^{\frac{1}{2}} + 5 \left( \frac{1}{4} + \frac{1}{4} \right)^{\frac{1}{2}} + 4 \left( \frac{1}{3} + \frac{1}{6} \right)^{\frac{1}{2}} + 6 \left( \frac{1}{4} + \frac{1}{5} \right)^{\frac{1}{2}} + 3 \left( \frac{1}{5} + \frac{1}{5} \right)^{\frac{1}{2}} + 10 \left( \frac{1}{5} + \frac{1}{6} \right)^{\frac{1}{2}} + 3 \left( \frac{1}{5} + \frac{1}{7} \right)^{\frac{1}{2}} + 11 \left( \frac{1}{6} + \frac{1}{6} \right)^{\frac{1}{2}} + 1 \left( \frac{1}{5} + \frac{1}{8} \right)^{\frac{1}{2}} + 3 \left( \frac{1}{6} + \frac{1}{7} \right)^{\frac{1}{2}} + 2 \left( \frac{1}{6} + \frac{1}{8} \right)^{\frac{1}{2}} = 84.63$

d)  $IN2(H) = \sum_{st \in E(H)} \left( \frac{1}{d(s)} + \frac{1}{d(t)} \right)^{-\frac{1}{2}} = 9 \left( \frac{1}{1} + \frac{1}{3} \right)^{-\frac{1}{2}} + 13 \left( \frac{1}{2} + \frac{1}{2} \right)^{-\frac{1}{2}} + 26 \left( \frac{1}{2} + \frac{1}{3} \right)^{-\frac{1}{2}} + 5 \left( \frac{1}{3} + \frac{1}{3} \right)^{-\frac{1}{2}} + 5 \left( \frac{1}{3} + \frac{1}{5} \right)^{-\frac{1}{2}} + 5 \left( \frac{1}{4} + \frac{1}{4} \right)^{-\frac{1}{2}} + 4 \left( \frac{1}{3} + \frac{1}{6} \right)^{-\frac{1}{2}} + 6 \left( \frac{1}{4} + \frac{1}{5} \right)^{-\frac{1}{2}} + 3 \left( \frac{1}{5} + \frac{1}{5} \right)^{-\frac{1}{2}} + 10 \left( \frac{1}{5} + \frac{1}{6} \right)^{-\frac{1}{2}} + 3 \left( \frac{1}{5} + \frac{1}{7} \right)^{-\frac{1}{2}} + 11 \left( \frac{1}{6} + \frac{1}{6} \right)^{-\frac{1}{2}} + 1 \left( \frac{1}{5} + \frac{1}{8} \right)^{-\frac{1}{2}} + 3 \left( \frac{1}{6} + \frac{1}{7} \right)^{-\frac{1}{2}} + 2 \left( \frac{1}{6} + \frac{1}{8} \right)^{-\frac{1}{2}} = 140.2006$



### 3.6. Arbidol

Arbidol, also known as umifenovir, is an antiviral medication initially developed in Russia and China. It is used for the treatment of respiratory viral infections and has gained considerable attention in the context of COVID-19. Figure 6 displays arbidol's molecular graph. Table 6 demonstrates the edge partition according to degree. This structure has 29 vertices and 31 edges (see Figure 6).

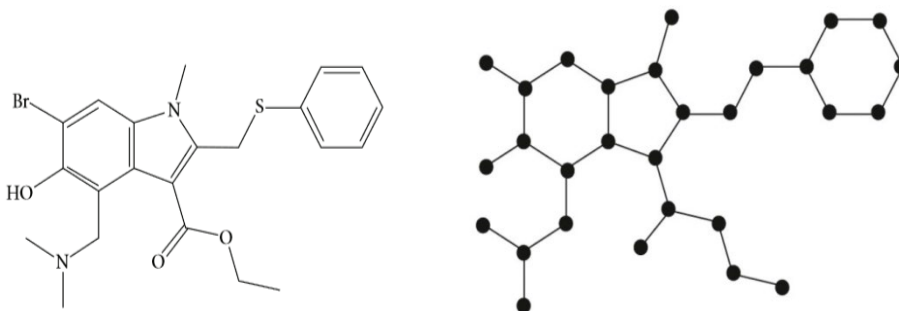


**Figure 6.** Arbidol 's Molecular Graph

**Table 6.** Edge Partitioning of Arbidol Based on Degree

$(d_2(s), d_2(t))$	Frequency
(1,2)	1
(1,3)	6
(2,2)	6
(2,3)	10
(3,3)	9
(3,4)	2
(3,5)	1
(4,4)	2
(3,6)	2
(4,5)	2
(3,7)	2
(4,6)	1
(5,5)	1
(5,6)	4
(6,6)	1
(5,8)	1

$(d_2(s), d_2(t))$	Frequency
(6,7)	1
(6,8)	2
(7,8)	3
(6,9)	1
(8,9)	3
(9,9)	1

**Theorem 3.6.** Nirmala leap index, modified Nirmala leap index, first inverse Nirmala index, and second inverse Nirmala index for arbidol are as follows:

- $NL(H) = 172.0932$ ,
- $mNL(H) = 23.7187$ ,
- $IN1(H) = 48.9311$ ,
- $IN2(H) = 87.20$ .

**Proof.** By using the degree-based edge partition and definitions, we may conclude that

$$\begin{aligned} \text{a) } NL(H) &= \sum_{st \in E(H)} [d(s) + d(t)]^{1/2} = 1(1 + 2)^{1/2} + 6(1 + 3)^{1/2} + \\ &6(2 + 2)^{1/2} + 10(2 + 3)^{1/2} + 9(3 + 3)^{1/2} + 2(3 + 4)^{1/2} + 1(3 + \\ &5)^{1/2} + 2(4 + 4)^{1/2} + 2(3 + 6)^{1/2} + 2(4 + 5)^{1/2} + 2(3 + 7)^{1/2} + 1(4 + \\ &6)^{1/2} + 1(5 + 5)^{1/2} + 4(5 + 6)^{1/2} + 1(6 + 6)^{1/2} + 1(5 + 8)^{1/2} + 1(6 + \\ &7)^{1/2} + 2(6 + 8)^{1/2} + 3(7 + 8)^{1/2} + 1(6 + 9)^{1/2} + 3(8 + 9)^{1/2} + 1(9 + \\ &9)^{1/2} = 172.0932 \end{aligned}$$

$$\begin{aligned} \text{b) } mNL(H) &= \sum_{st \in E(H)} \frac{1}{\sqrt{d(s)+d(t)}} = 1(1 + 2)^{-1/2} + 6(1 + 3)^{-1/2} + 6(2 + \\ &2)^{-1/2} + 10(2 + 3)^{-1/2} + 9(3 + 3)^{-1/2} + 2(3 + 4)^{-1/2} + 1(3 + \\ &5)^{-1/2} + 2(4 + 4)^{-1/2} + 2(3 + 6)^{-1/2} + 2(4 + 5)^{-1/2} + 2(3 + 7)^{-1/2} + \\ &1(4 + 6)^{-1/2} + 1(5 + 5)^{-1/2} + 4(5 + 6)^{-1/2} + 1(6 + 6)^{-1/2} + 1(5 + \\ &8)^{-1/2} + 1(6 + 7)^{-1/2} + 2(6 + 8)^{-1/2} + 3(7 + 8)^{-1/2} + 1(6 + 9)^{-1/2} + \\ &3(8 + 9)^{-1/2} + 1(9 + 9)^{-1/2} = 23.7187 \end{aligned}$$

$$\begin{aligned} \text{c) } IN1(H) &= \sum_{st \in E(H)} \left( \frac{1}{d(s)} + \frac{1}{d(t)} \right)^{\frac{1}{2}} = 1 \left( \frac{1}{1} + \frac{1}{2} \right)^{\frac{1}{2}} + 6 \left( \frac{1}{1} + \frac{1}{3} \right)^{\frac{1}{2}} + 6 \left( \frac{1}{2} + \right. \\ &\left. \frac{1}{2} \right)^{\frac{1}{2}} + 10 \left( \frac{1}{2} + \frac{1}{3} \right)^{\frac{1}{2}} + 9 \left( \frac{1}{3} + \frac{1}{3} \right)^{\frac{1}{2}} + 2 \left( \frac{1}{3} + \frac{1}{4} \right)^{\frac{1}{2}} + 1 \left( \frac{1}{3} + \frac{1}{5} \right)^{\frac{1}{2}} + 2 \left( \frac{1}{4} + \frac{1}{4} \right)^{\frac{1}{2}} + \\ &2 \left( \frac{1}{3} + \frac{1}{6} \right)^{\frac{1}{2}} + 2 \left( \frac{1}{4} + \frac{1}{5} \right)^{\frac{1}{2}} + 2 \left( \frac{1}{3} + \frac{1}{7} \right)^{\frac{1}{2}} + 1 \left( \frac{1}{4} + \frac{1}{6} \right)^{\frac{1}{2}} + 1 \left( \frac{1}{5} + \frac{1}{5} \right)^{\frac{1}{2}} + 4 \left( \frac{1}{5} + \right. \end{aligned}$$

$$\left(\frac{1}{6}\right)^{\frac{1}{2}} + 1\left(\frac{1}{6} + \frac{1}{6}\right)^{\frac{1}{2}} + 1\left(\frac{1}{5} + \frac{1}{8}\right)^{\frac{1}{2}} + 1\left(\frac{1}{6} + \frac{1}{7}\right)^{\frac{1}{2}} + 2\left(\frac{1}{6} + \frac{1}{8}\right)^{\frac{1}{2}} + 3\left(\frac{1}{7} + \frac{1}{8}\right)^{\frac{1}{2}} + 1\left(\frac{1}{6} + \frac{1}{9}\right)^{\frac{1}{2}} + 3\left(\frac{1}{8} + \frac{1}{9}\right)^{\frac{1}{2}} + 1\left(\frac{1}{9} + \frac{1}{9}\right)^{\frac{1}{2}} = 48.9311$$

$$\text{d) } IN2(H) = \sum_{st \in E(H)} \left(\frac{1}{d(s)} + \frac{1}{d(t)}\right)^{-\frac{1}{2}} = 1\left(\frac{1}{1} + \frac{1}{2}\right)^{-\frac{1}{2}} + 6\left(\frac{1}{1} + \frac{1}{3}\right)^{-\frac{1}{2}} + 6\left(\frac{1}{2} + \frac{1}{2}\right)^{-\frac{1}{2}} + 10\left(\frac{1}{2} + \frac{1}{3}\right)^{-\frac{1}{2}} + 9\left(\frac{1}{3} + \frac{1}{3}\right)^{-\frac{1}{2}} + 2\left(\frac{1}{3} + \frac{1}{4}\right)^{-\frac{1}{2}} + 1\left(\frac{1}{3} + \frac{1}{5}\right)^{-\frac{1}{2}} + 2\left(\frac{1}{4} + \frac{1}{4}\right)^{-\frac{1}{2}} + 2\left(\frac{1}{3} + \frac{1}{6}\right)^{-\frac{1}{2}} + 2\left(\frac{1}{4} + \frac{1}{5}\right)^{-\frac{1}{2}} + 2\left(\frac{1}{3} + \frac{1}{7}\right)^{-\frac{1}{2}} + 1\left(\frac{1}{4} + \frac{1}{6}\right)^{-\frac{1}{2}} + 1\left(\frac{1}{5} + \frac{1}{5}\right)^{-\frac{1}{2}} + 4\left(\frac{1}{5} + \frac{1}{6}\right)^{-\frac{1}{2}} + 1\left(\frac{1}{6} + \frac{1}{6}\right)^{-\frac{1}{2}} + 1\left(\frac{1}{5} + \frac{1}{8}\right)^{-\frac{1}{2}} + 1\left(\frac{1}{6} + \frac{1}{7}\right)^{-\frac{1}{2}} + 2\left(\frac{1}{6} + \frac{1}{8}\right)^{-\frac{1}{2}} + 3\left(\frac{1}{7} + \frac{1}{8}\right)^{-\frac{1}{2}} + 1\left(\frac{1}{6} + \frac{1}{9}\right)^{-\frac{1}{2}} + 3\left(\frac{1}{8} + \frac{1}{9}\right)^{-\frac{1}{2}} + 1\left(\frac{1}{9} + \frac{1}{9}\right)^{-\frac{1}{2}} = 87.20$$

#### 4. COMPARITIVE ANALYSIS OF COMPUTED TIS

We now perform a comparative analysis of the computed T Is for each medicine and for each index.

##### 4.1. Remdesivir

Remdesivir's comparatively high Nirmala leap index ( $NL(H)$ ) value of 246.3012 suggests that it has a notable effect or potency. The modified Nirmala leap index ( $mNL(H)$ ) value is 33.3229, indicating a diminished but discernible influence following the adjustments. With 69.0372 as the first inverse Nirmala index ( $IN1(H)$ ) value, mild inverse qualities are reflected. With a greater value of 119.9954 for the second inverse Nirmala index ( $IN2(H)$ ) than the first, strong inverse qualities are indicated.

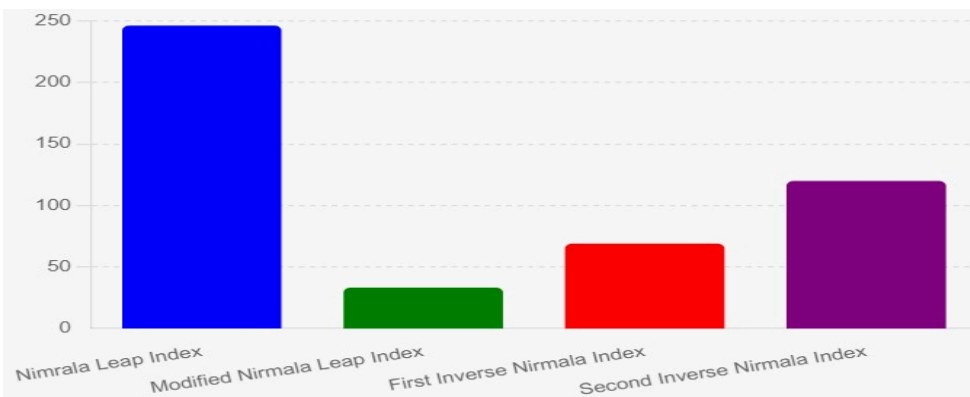
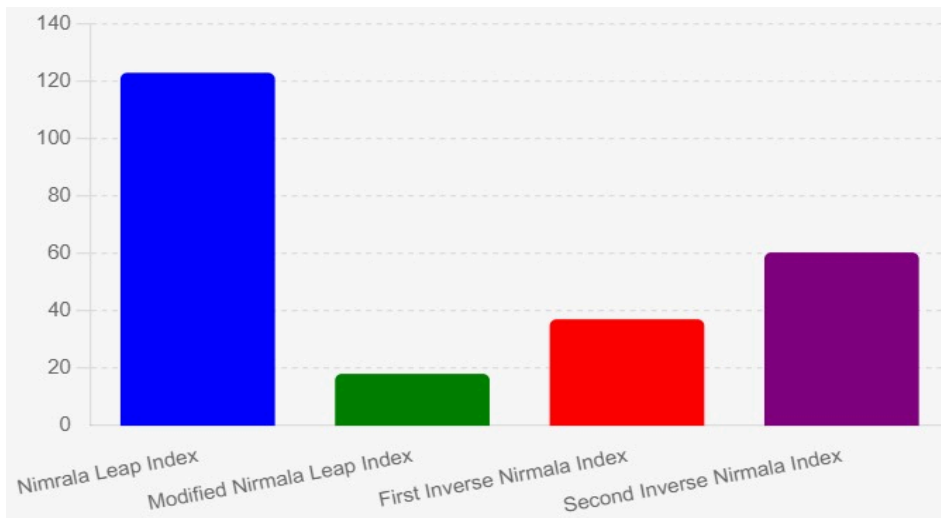


Figure 7. Comparitive Analysis of Remdesivir

## 4.2. Chloroquine

Compared to remdesivir, chloroquine has a lower Nimrala leap index ( $NL(H)$ ) value of 123.004, indicating less potency or impact. Following changes, the modified Nirmala leap index ( $mNL(H)$ ) value is 18.1063, showing a considerable reduction in impact. With a lower inverse property of 37.1161, the first inverse Nirmala index ( $IN1(H)$ ) is displayed. Compared to remdesivir, the value of second inverse Nirmala index ( $IN2(H)$ ) is comparatively low at 60.3967, suggesting lower inverse properties.



**Figure 8.** Comparitive Analysis of Chloroquine

## 4.3. Hydroxychloroquine

Similar to chloroquine but slightly more potent, hydroxychloroquine has a Nimrala leap index ( $NL(H)$ ) value of 127.7733. After changes, the modified Nirmala leap index ( $mNL(H)$ ) value is 18.9840, indicating a decrease in impact. There are moderate inverse properties, as shown by the first inverse Nirmala index ( $IN1(H)$ ) value of 38.8533. Strong inverse characteristics are suggested by the second inverse Nirmala index ( $IN2(H)$ ) value of 62.8089, which is marginally greater than that of chloroquine.

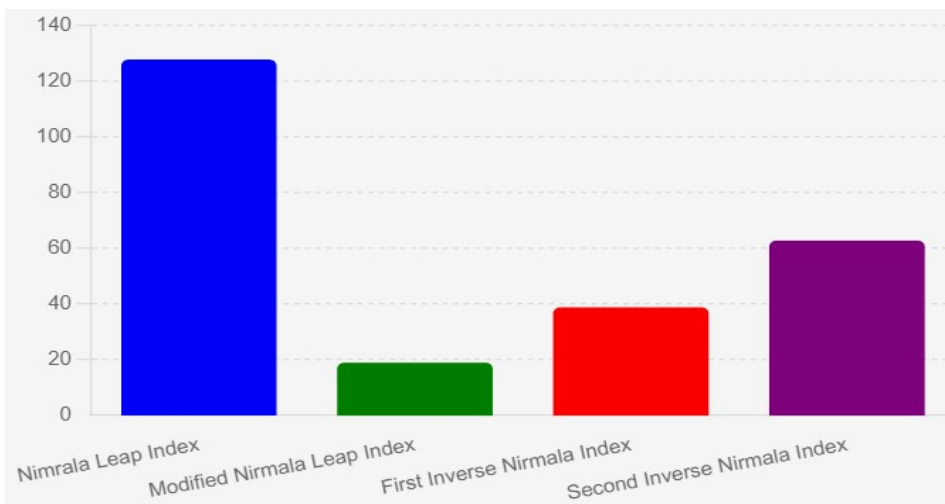


**Figure 9.** Comparative Analysis of Hydroxychloroquine

#### 4.4. Theaflavin

Theaflavin has a notable potency, as evidenced by its high Nimrala leap index ( $NL(H)$ ) value of 265.5221. The modified Nimrala leap index ( $mNL(H)$ ) value is 33.7404, which indicates a noteworthy but significant decrease following the adjustments. With a first inverse Nimrala index ( $IN1(H)$ ) value of 69.9288, strong inverse characteristics are indicated. With a high value of 129.7463, the second inverse Nimrala index ( $IN2(H)$ ) indicates strong inverse qualities.

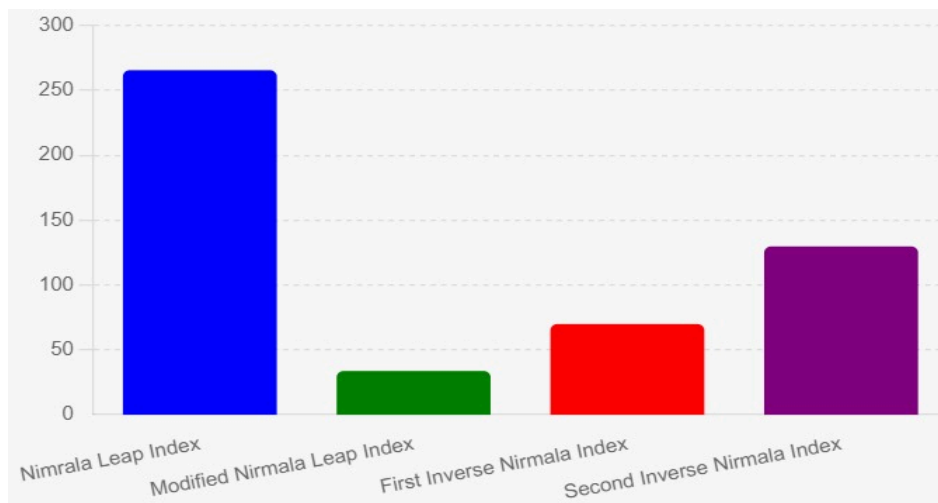


**Figure 10.** Comparative Analysis of Theaflavin

#### 4.5. Ritonavir

With a Nimrala leap index ( $NL(H)$ ) value of 285.7254, ritonavir has the highest comparative potency or impact of all the medications. At 41.1869, the modified Nirmala leap index ( $mNL(H)$ ) value indicates a noteworthy decrease. With a value of 84.63, the first inverse Nirmala index ( $IN1(H)$ ) shows significant inverse characteristics. With the highest value among the medications compared, the second inverse Nirmala index ( $IN2(H)$ ) is 140.2006, suggesting very strong inverse characteristics.

#### 4.6. Arbidol

Arbidol's moderate Nimrala leap index ( $NL(H)$ ) value of 172.0932 indicates a notable but not very significant potency. After changes, the modified Nirmala leap index ( $mNL(H)$ ) value is 23.7187, indicating a decrease in impact. There are moderate inverse properties, as shown by the first inverse Nirmala index ( $IN1(H)$ ) value of 48.9311. The modest second inverse Nirmala index ( $IN2(H)$ ) value of 87.2083 indicates passable but not particularly strong inverse qualities.

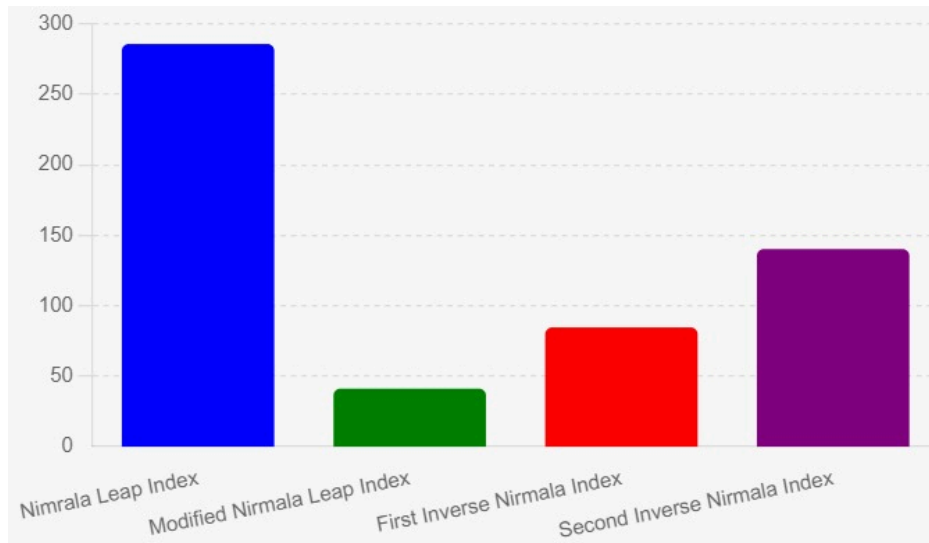


**Figure 11.** Comparative Analysis of Ritonavir

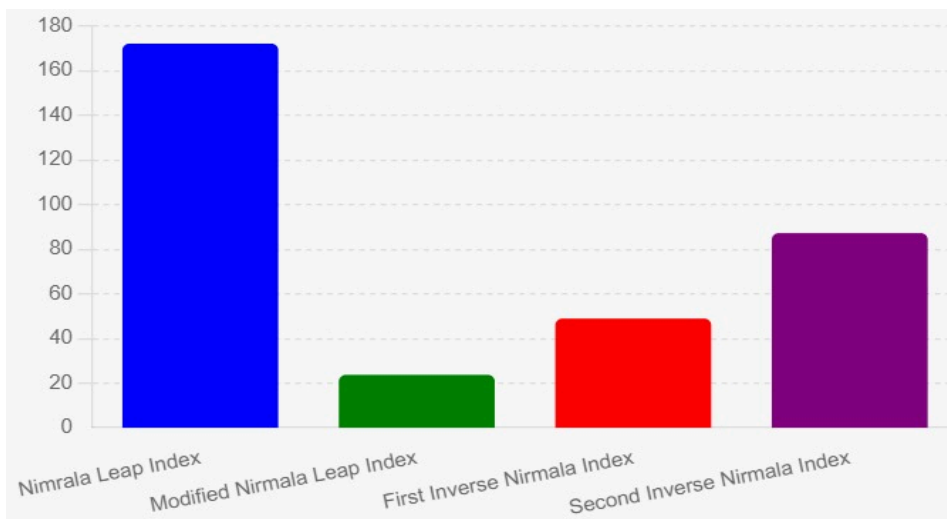


**Figure 12.** Comparative Analysis of Arbidol

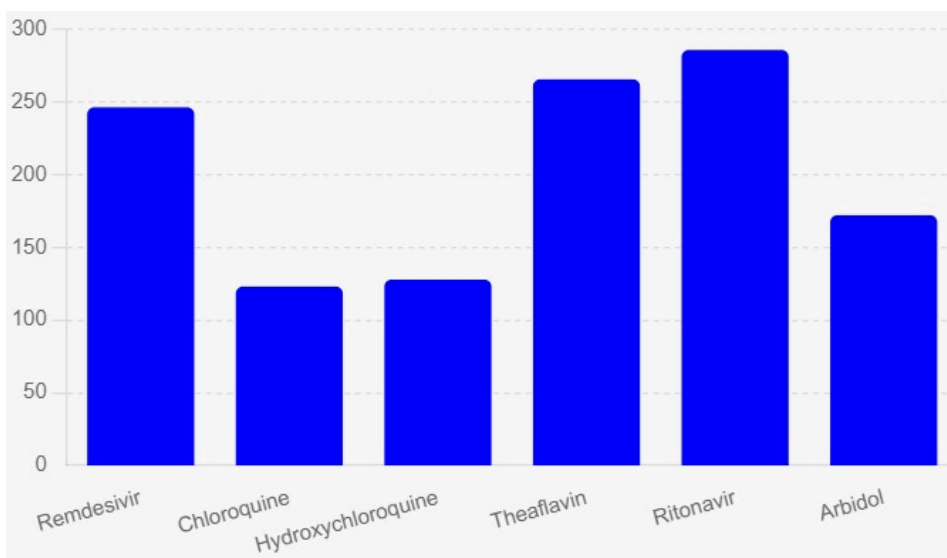


**Figure 13.** Comparative Analysis of Nimrala Leap Index

#### 4.7. Nimrala Leap Index ( $NL(H)$ )

The relative potencies of the medicines under consideration are disclosed by the Nimrala leap index ( $NL(H)$ ). With an  $NL(H)$  value of 246.3012, remdesivir is the second most potent drug after ritonavir and theaflavin, suggesting a strong effect or efficacy. Conversely, of the

medicines compared, chloroquine has the lowest  $NL(H)$  value of 123.004, indicating that it has the least influence. With an  $NL(H)$  value of 127.7733, hydroxychloroquine exhibits a somewhat higher potency than chloroquine, suggesting a moderate level of efficacy. Further, with a notable  $NL(H)$  of 265.5221, theaflavin is second only to ritonavir, which has the highest  $NL(H)$  value of 285.7254, signifying the most potency or impact. Arbidol also shows a notable effect, though not as much as ritonavir or theaflavin, with an  $NL(H)$  value of 172.0932.

#### 4.8. Modified Nirmala Leap Index ( $mNL(H)$ )

Understanding how changes affect the potency of various medicines is possible with the help of the modified Nirmala leap index ( $mNL(H)$ ). Remdesivir's  $mNL(H)$  value of 33.3229 suggests a diminished but noteworthy effect in comparison to its  $NL(H)$ . With the lowest  $mNL(H)$  value of 18.1063, chloroquine appears to be the least impacted by the changes. The  $mNL(H)$  value of 18.9840 for hydroxychloroquine is marginally higher, suggesting a minor increase in effect following modification. Theaflavin shows a notable but considerable reduction in impact, with an  $mNL(H)$  value of 33.7404. Ritonavir has the highest  $mNL(H)$  value of 41.1869, indicating that changes do not affect its potency. Following changes, arbidol exhibits a moderate reduction in impact with an  $mNL(H)$  value of 23.7187.

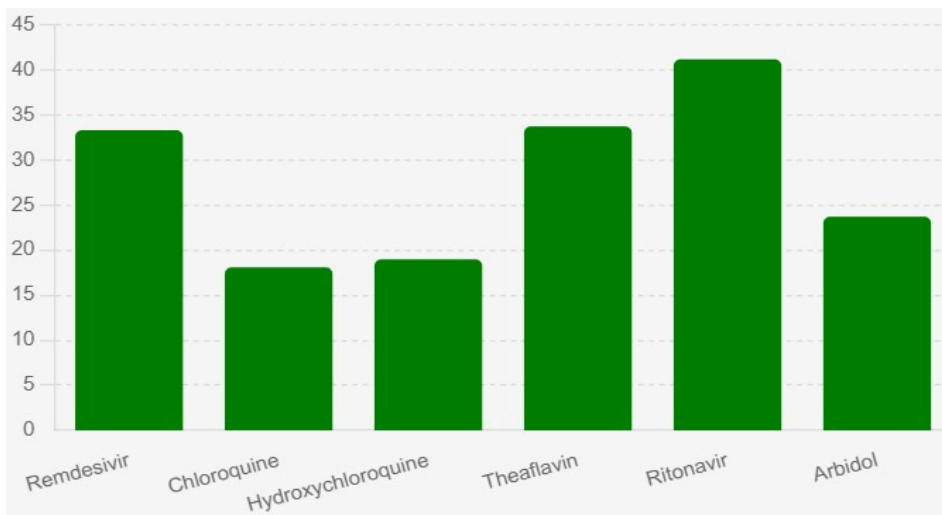


**Figure 14.** Comparative Analysis of Modified Nirmala Leap Index



#### 4.9. First Inverse Nirmala Index ( $IN1(H)$ )

The inverse characteristics of the medicines are measured by using the first inverse Nirmala index ( $IN1(H)$ ). Remdesivir exhibits modest inverse characteristics, as indicated by its  $IN1(H)$  value of 69.0372. Chloroquine has lesser inverse characteristics, as seen by its lowest  $IN1(H)$  value of 37.1161. Compared to chloroquine, hydroxychloroquine has slightly higher inverse characteristics, with an  $IN1(H)$  value of 38.8533. Theaflavin exhibits strong inverse characteristics, as evidenced by its  $IN1(H)$  value of 69.9288. Ritonavir has the strongest inverse characteristics among the medicines examined, with the highest  $IN1(H)$  value of 84.63. Arbidol exhibits moderate inverse characteristics, as indicated by its  $IN1(H)$  value of 48.9311.

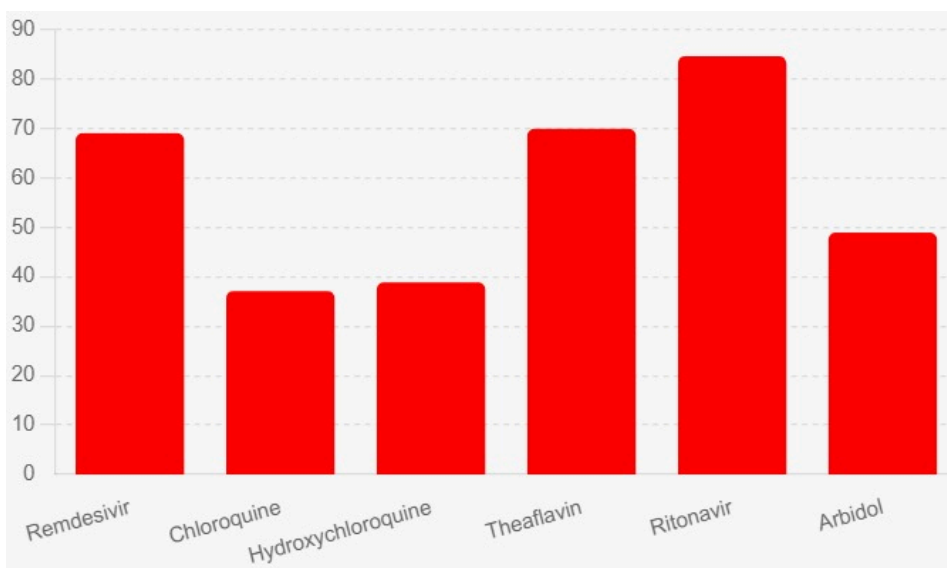


**Figure 15.** First Inverse Nirmala Index

#### 4.10. Second Inverse Nirmala Index ( $IN2(H)$ )

The medicines' inverse qualities are assessed further by the second inverse Nirmala index ( $IN2(H)$ ). Remdesivir exhibits high inverse characteristics, as evidenced by its  $IN2(H)$  value of 119.9954. With the lowest  $IN2(H)$  score of 60.3967, chloroquine is indicative of inverse characteristics that are less strong. Compared to chloroquine, hydroxychloroquine shows slightly higher inverse characteristics, with an

$IN2(H)$  value of 62.8089. Ritonavir is slightly ahead of theaflavin in strong inverse characteristics, having an  $IN2(H)$  value of 129.7463. Among all the medicines compared, ritonavir has the strongest inverse characteristics, with the highest  $IN2(H)$  value of 140.2006. Despite having a moderate inverse ( $IN2(H)$ ) value of 87.2083, arbidol is more potent than hydroxychloroquine and chloroquine.

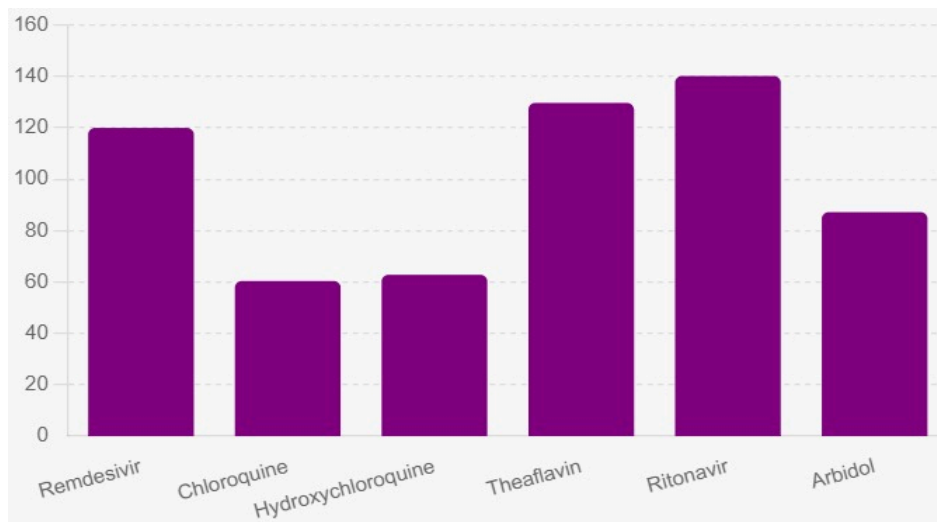


**Figure 16.** Second Inverse Nirmala Index

## 5. CONCLUSION AND FUTURE RESEARCH

The Nirmala leap index, modified Nirmala leap index, first inverse Nirmala index, and second inverse Nirmala index of selected antiviral medicines used to treat COVID-19, including remdesivir, arbidol, theaflavin, ritonavir, chloroquine, and hydroxychloroquine, were examined in this study. According to the findings, TIs play a crucial role in assessing the structural characteristics of these substances and offering information about their possible potency and efficacy. For example, ritonavir has the greatest Nirmala leap index value when compared to other medicines under study, indicating that it has better structural stability and potential antiviral application. The potential use of these TIs in Quantitative Structure-Property Relationship (QSPR) analysis is the most important finding of this research. We are able to forecast the behavior and effectiveness of these medicines in various environments by establishing a connection between these indices and other physiochemical characteristics, such as critical

pressure, enthalpy, and boiling points. Extending this analysis to a wider spectrum of antiviral drugs and investigating their QSPR models should be the main goals of future research. Future research should also look into how these indices can be used in the development of novel antiviral medications, especially those that target newly developing viral strains.

### CONFLICT OF INTEREST

The authors of the manuscript have no financial or non-financial conflict of interest in the subject matter or materials discussed in this manuscript.

### DATA AVAILABILITY STATEMENT

The data associated with this study will be provided by the corresponding author upon request.

### FUNDING DETAILS

No funding has been received for this research.

### REFERENCES

1. Huang C, Wang Y, Li X, et al. Clinical features of patients infected with 2019 novel coronavirus in Wuhan, China. *Lancet*. 2020;395(10223):497–506. [https://doi.org/10.1016/S0140-6736\(20\)30183-5](https://doi.org/10.1016/S0140-6736(20)30183-5)
2. Zhou D, Dai SM, Tong Q. COVID-19: a recommendation to examine the effect of hydroxychloroquine in preventing infection and progression. *J Antimicro Chemother*. 2020;75(7):1667–1670. <https://doi.org/10.1093/jac/dkaa114>
3. Morse JS, Lalonde T, Xu S, Liu WR. Learning from the past: possible urgent prevention and treatment options for severe acute respiratory infections caused by 2019-nCoV. *Chembiochem*. 2020;21(5):730–738. <https://doi.org/10.1002/cbic.202000047>
4. Lung J, Lin YS, Yang YH, et al. The potential chemical structure of anti-SARS-CoV-2 RNA-dependent RNA polymerase. *J Med Virol*. 2020;92(6):693–697. <https://doi.org/10.1002/jmv.25761>
5. Wang M, Cao R, Zhang L, et al. Remdesivir and chloroquine effectively inhibit the recently emerged novel coronavirus (2019-nCoV) in vitro. *Cell Res*. 2020;30(3):269–271. <https://doi.org/10.1038/s41422-020-0282-0>

6. Xu X, Chen P, Wang J, et al. Evolution of the novel coronavirus from the ongoing Wuhan outbreak and modeling of its spike protein for risk of human transmission. *Sci China Life Sci.* 2020;63:457–460. <https://doi.org/10.1007/s11427-020-1637-5>
7. Farman M, Akgül A, Nisar KS, et al. Epidemiological analysis of fractional order COVID-19 model with Mittag-Leffler kernel. *AIMS Math.* 2022;7(1):756–783. <https://doi.org/10.3934/math.2022046>
8. Warren TK, Jordan R, Lo MK, et al. Therapeutic efficacy of the small molecule GS-5734 against Ebola virus in rhesus monkeys. *Nature.* 2016;531(7594):381–385. <https://doi.org/10.1038/nature17180>
9. Hu M, Ali H, Binyamin MA, Ali B, Liu JB, Fan C. On distance-based topological descriptors of chemical interconnection networks. *J Math.* 2021;2021(1):e5520619. <https://doi.org/10.1155/2021/5520619>
10. Savarino A, Di Trani L, Donatelli I, Cauda R, Cassone A. New insights into the antiviral effects of chloroquine. *Lancet Infect Dis.* 2006;6(2):67–69. [https://doi.org/10.1016/s1473-3099\(06\)70361-9](https://doi.org/10.1016/s1473-3099(06)70361-9)
11. Yan Y, Zou Z, Sun Y, et al. Anti-malaria drug chloroquine is highly effective in treating avian influenza A H5N1 virus infection in an animal model. *Cell Res.* 2013;23(2):300–302. <https://doi.org/10.1038/cr.2012.165>
12. Khan A, Zarin R, Humphries UW, Akgül A, Saeed A, Gul T. Fractional optimal control of COVID-19 pandemic model with generalized Mittag-Leffler function. *Adv Difference Equat.* 2021;2021:1–22. <https://doi.org/10.1186/s13662-021-03546-y>
13. Amin M, Farman M, Akgül A, Alqahtani RT. Effect of vaccination to control COVID-19 with fractal fractional operator. *Alexand Eng J.* 2022;61(5):3551–3557. <https://doi.org/10.1016/j.aej.2021.09.006>
14. Azeem M, Aslam A, Iqbal Z, Binyamin MA, Gao W. Topological aspects of 2D structures of trans-Pd (NH<sub>2</sub>) S lattice and a metal-organic superlattice. *Arab J Chem.* 2021;14(3):e102963. <https://doi.org/10.1016/j.arabjc.2020.102963>
15. Chowdhury P, Sahuc ME, Rouillé Y, et al. Theaflavins, polyphenols of black tea, inhibit entry of hepatitis C virus in cell culture. *PLoS One.* 2018;13(11):e0198226. <https://doi.org/10.1371/journal.pone.0198226>

16. Yang ZF, Bai LP, Huang WB, et al. Comparison of in vitro antiviral activity of tea polyphenols against influenza A and B viruses and structure–activity relationship analysis. *Fitoterapia*. 2014;93:47–53. <https://doi.org/10.1016/j.fitote.2013.12.011>
17. Wiener H. Structural determination of paraffin boiling points. *J Am Chem Soc*. 1947;69(1):17–20. <https://doi.org/10.1021/ja01193a005>
18. Gutman I, Polansky OE. *Mathematical Concepts in Organic Chemistry*. Springer Science & Business Media; 2012. <https://doi.org/10.1007/978-3-642-70982-1>
19. Trinajstić N. *Chemical Graph Theory*. CRC Press; 2018. <https://doi.org/10.1201/9781315139111>
20. Kulli VR. Nirmala index. *Int J Math Trends Technol*. 2021;67(3):eIJMTT-V67I3P502. <https://doi.org/10.14445/22315373/IJMTT-V67I3P502>
21. Basak SC, Niemi GJ, Veith GD. Predicting properties of molecules using graph invariants. *J Math Chem*. 1991;7(1):243–272. <https://doi.org/10.1007/BF01200826>
22. Dai YM, Zhu ZP, Cao Z, Zhang YF, Zeng JL, Li X. Prediction of boiling points of organic compounds by QSPR tools. *J Molecul Graph Model*. 2013;44:113–119. <https://doi.org/10.1016/j.jmgm.2013.04.007>
23. Amin S, Rehman MA, Farahani MR, Cancan M, Aldemir MS. Multiplicative degree-based topological indices and line graph of hex board graph. *Eurasian Chem Commun*. 2020;2(11):1137–1145. <https://doi.org/10.22034/ecc.2020.255142.1093>
24. Amin S, Rehman MA, Farahani MR, Cancan M, Aldemir MS. M-polynomial and degree-based topological indices and line graph of hex board graph. *Eurasian Chem Commun*. 2020;2(12):1156–1163. <https://doi.org/10.22034/ecc.2020.255143.1094>
25. Amin S, Rehman Virk AU, Rehman MA, Shah NA. Analysis of dendrimer generation by Sombor indices. *J Chem*. 2021;2021(1):e9930645. <https://doi.org/10.1155/2021/9930645>
26. Gutman I, Kulli VR. Nirmala energy. *Open J Disc Appl Math*. 2021;4(2):11–16.

27. Kulli VR, Gutman I. On some mathematical properties of Nirmala index. *Ann Pure Appl Math.* 2021;23(2):93–99. <https://doi.org/10.22457/apam.v23n2a06822>
28. Kulli VR, Harish N, Chaluvvaraju B. Sombor leap indices of some chemical drugs. *RES Rev Int J Multidiscip.* 2022;7(10):158–166. <https://doi.org/10.31305/rrijm.2022.v07.i10.019>
29. Kulli VR. Different versions of Nirmala index of certain chemical structures. *Int J Math Trends Technol.* 2021;67(7):eIJMTT-V67I7P507. <https://doi.org/10.14445/22315373/IJMTT-V67I7P507>
30. Kulli VR, Loksha V, Nirupadi K. Computation of inverse Nirmala indices of certain nanostructures. *Int J Math Combin.* 2021;2:33–40. <https://doi.org/10.22457/apam.v23n2a02821>